FULL 3D SEISMIC RESPONSE ANALYSIS OF UNDERGROUND RAMP TUNNEL STRUCTURE USING LARGE-SCALE NUMERICAL COMPUTATION

H. Dobashi [1], T. Hatsuku[2], T. Ichimura[3], M. Hori[4], T. Yamada[5], N. Ohbo[5], M. Moriguchi[6] and H. Itami[5]

[1] *Manager, Construction Management Division, Metropolitan Expressway Co., Ltd., Tokyo, Japan*
Email: h.dobashi118@shutoko.jp
[2] *Senior Engineer , Tokyo Construction Bureau, Metropolitan Expressway Co., Ltd., Tokyo, Japan*
Email: t.hatsuku811@shutoko.jp
[3] *Associate Professor, Department of Civil and Environmental Engineering, Tokyo Institute of Technology, Tokyo, Japan*
Email: ichimura@cv.titech.ac.jp
[4] *Professor, Earthquake Research Institute, University of Tokyo, Tokyo, Japan*
Email: hori@eri.u-tokyo.ac.jp
[5] *Chief Senior Research Engineer , Kajima Technical Research Institute, Kajima Corp., Tokyo, Japan*
Email: takemine@kajima.com, ohbo@kajima.com, itamihi@kajima.com
[6] *Director, Construction Office, Tokyo Construction Branch, Kajima Corp., Tokyo, Japan*
Email: moriguchi@kajima.com

ABSTRACT :

In the Tokyo metropolitan area, long tunnels are being constructed to make a ring road network. These long tunnels need a ramp tunnel which connects the main tunnel located deep underground to ground level. However, ramp tunnels have a complicated structure and their seismic behavior cannot accurately be evaluated by 2D analysis, therefore a precise examination by 3D analysis is required. In the present study we make a detailed model of the soil-structure system of the ramp tunnel and conduct large-scale numerical computation for the 3D seismic response analysis using a dynamic elastic FEM. The major findings are as follows: i) deformation of the ramp tunnel is not accurately estimated by the standard 2D analysis; ii) the seismic response of the main tunnel is small in a hard soil layer and can be evaluated by the standard 2D analysis; and iii) the 3D seismic response of the ramp tunnel significantly changes depending on the characteristics of the input earthquake ground motion.

KEYWORDS: underground structure, large-scale computation, FEM, seismic response analysis

1. INTRODUCTION

The Great Hanshin Earthquake of January 1995 caused great damage to underground structures, highlighting the need for seismic design which takes into account the dynamic behavior of underground structures, particularly structures whose configurations change significantly or which are located in complex ground structures. Observation and dynamic analyses seeking to clarify the seismic behavior of such underground structures have long been performed, but little attention has been paid to the analysis method used for the seismic design, and a numerical seismic design method has not yet been established.

According to the Act on Temporary Measures concerning Public Use of the Deep Underground enforced in April 2001, there are plans to construct expressways and railroads deep underground in the Tokyo metropolitan area. As part of the project to construct three metropolitan loop expressways, construction of the Yamate Tunnel for the Metropolitan Expressway Central Circular Line, which is an underground tunnel with a large cross-section, has been started. For this underground expressway, ramp tunnels have to be provided to connect the surface level to the main tunnel. The structure of such ramp tunnels is complicated: it is a joint with the main tunnel, going upwards to the surface after passing through multiple sedimentary layers. The ramp tunnel is expected to behave in a complex manner during an earthquake (Ohbo et al., 2004), yet the seismic design is still based on 2D analysis which may underestimate the complex seismic response of the ramp tunnel. An evaluation of the 3D seismic behavior of the ramp tunnel is required.

In the present study, we construct a detailed analysis model of the Yamate Tunnel and perform a large-scale numerical computation for the 3D seismic response analysis for varying input earthquake ground motions. To clarify the 3D behavior of the tunnel, we perform a 2D analysis for the cross section of the tunnel and compare the results with those obtained from the 3D analysis.

2. SCOPE OF ANALYSIS

The numerical analysis is performed for the Nishi Shinjuku South Junction Tunnel of the Yamate Tunnel as shown in Figure 1. The structure has a center ramp system consisting of two main tunnels (outside diameter 12.83 m; lining thickness 0.53 m) and an exit/entrance tunnel which connects the central part of the main tunnel with the ground surface. Accordingly, the ramp tunnel structure changes with a divergence/confluence part extending to the surface. The main tunnel is made of tunneling shields with large steel segments, while the exit/entrance tunnel is an RC structure with a rectangular section. The exit/entrance tunnel is constructed with the open-cut method to connect with the shield tunnel which is constructed earlier. Therefore, at the divergence/confluence section, the two tunnels with different types of structure and materials are to be joined.

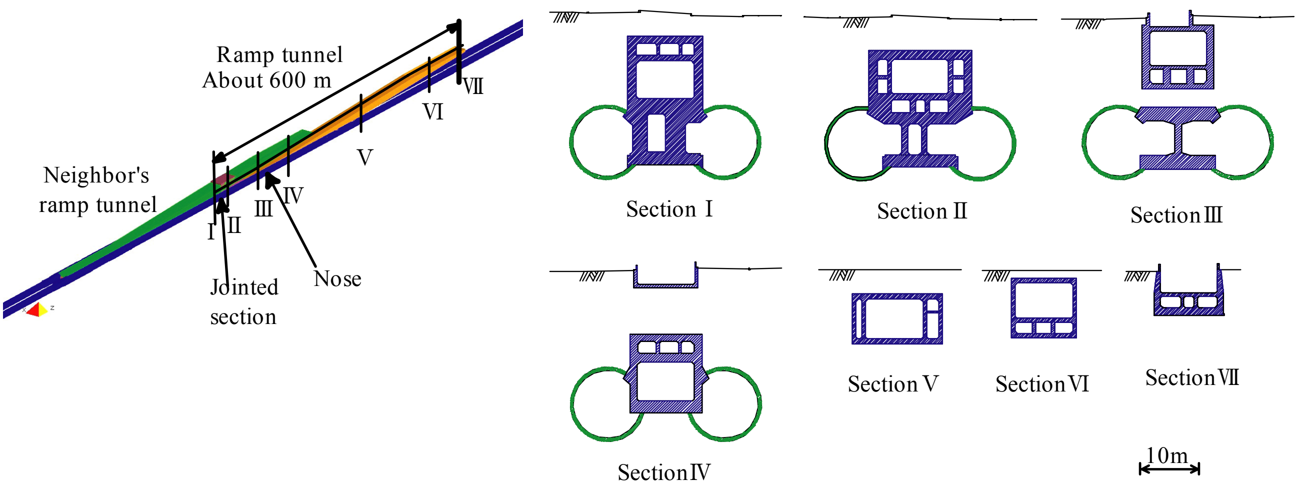

Figure 1 Overview of the Nishi Shinjuku South Junction

The ground structure which surrounds the tunnel system varies as illustrated in Figure 2. There is a sharp contrast in the shear wave velocity changes at the upper side of the Tokyo Gravel Layer, which is indicated as Tog in the figure: the average shear wave velocity of the upper sedimentary layer is 190 m/s, while that of the sedimentary layer below the Tokyo Gravel Layer is 490 m/s.

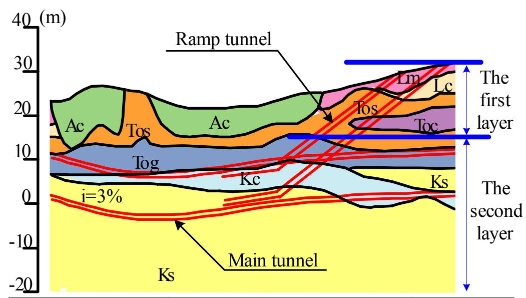

Geological feature	Alluvium	Kanto Loam layer		Tokyo layer Group			Kazusa layer Group	
Symbol	Ac	Lm	Lc	Tos	Toc	Tog	Kc	Ks

Figure 2 Vertical Section of Ground Structure

3. ANALYSIS METHOD

3.1 Modeling of Structure and Ground

The main tunnel is modeled as a uniform cylindrical structure; the cross-sectional shape is unchanged and the wall thickness is the same as the lining thickness of the steel segments. It is assumed that the tunnel is linearly elastic. Equivalent elastic moduli are used for the model so that the in-plane bending rigidity of the tunnel section coincides with that of the segments, and Poisson's ratio of the model is set the same as that of the steel material of the segments. A conversion value which agrees with the weight per unit length is used for the mass.

The ramp tunnel is modeled as a structure with a rectangular section; the width, height and thickness are 12.0 m, 8.5 m and 1.0 m, respectively. The model's alignment in the longitudinal cross section is a straight line with the same average gradient (= 7.4%) as that of the real structure. The elastic constant for RC structures (design standard strength σ_{ck} = 40 N/mm^2) is used as the analytic constant.

The ground is modeled as a two horizontal layer structure. Equivalent rigidity and damping ratio are used; this setting is the same as the actual design, since the dynamic elastic analysis analogously assumes that the ground is non-linear.

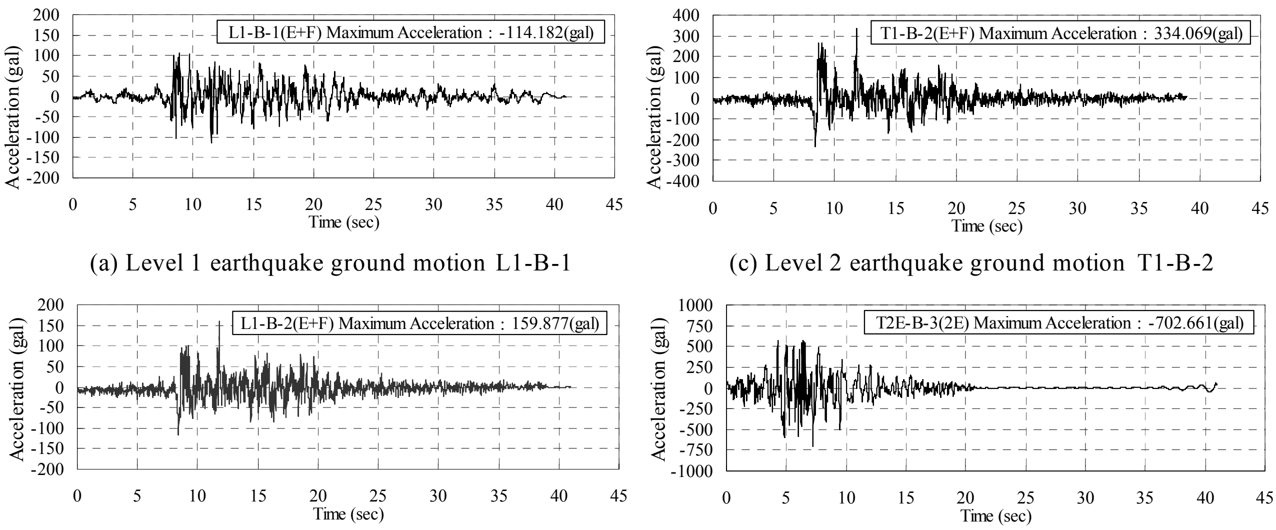

(a) Level 1 earthquake ground motion L1-B-1
(c) Level 2 earthquake ground motion T1-B-2
(b) Level 1 earthquake ground motion L1-B-2
(d) Level 2 earthquake ground motion T2E-B-3

Figure 3 Input Earthquake Ground Motion: Design Wave

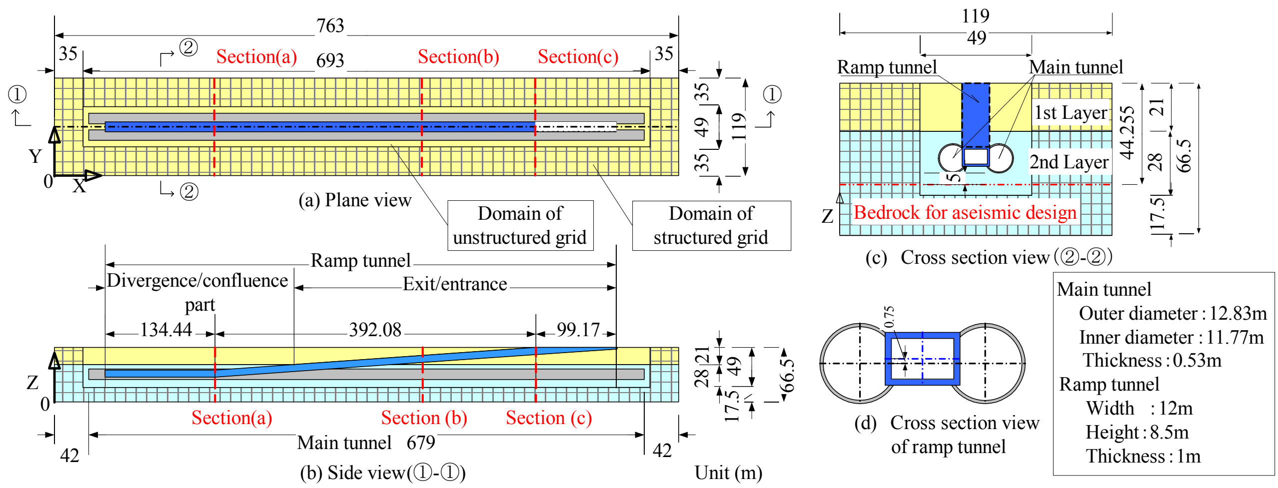

Figure 4 3D Model for the Numerical Analysis

Table 1 Analytical Parameters

		Unit weight ρ (kg/m^3)	Shear wave velocity Vs (m/s)	Poisson's ratio ν (-)	Damping constant*1 α (-)	Remarks
L1 earthquake ground Motion	Main tunnel	609	3372	0.30	0.9	*2
	Ramp tunnel	2500	2299	0.15	0.9	*3
	First ground layer	1500	150	1.00	0.9	
	Second ground layer	2000	450	1.00	0.9	
L2 earthquake ground Motion	Main tunnel	609	3372	0.30	2.0	*2
	Ramp tunnel	2500	2299	0.15	2.0	*3
	First ground layer	1500	60	1.00	2.0	
	Second ground layer	2000	400	1.00	2.0	

*1: Mass proportional factor of Rayleigh damping *2: Conversion value of steel segments *3: RC structure(σ_{ck} = 40 N/mm^2)

For the numerical computation, seismic waves are inputted at 5 m below the bottom of the main tunnel (GL-34.255 m), which is the bedrock in the actual seismic design. As shown in Figure 3, four design earthquake ground motions which are used in the actual design are employed: two waves of Level 1 earthquake ground motion with a high probability of occurrence for structures in service, and two waves of Level 2 earthquake ground motion with a low probability but having a large acceleration.

Figure 4 illustrates the 3D model for the numerical analysis, and Table 1 summarizes the parameters used for the Level 1 and 2 cases. The distance from the tunnel to the model boundary is set sufficiently long and wide; this is necessary to decrease the effects of the artificial boundary on the structure's response, according to the results of previous study (Dobashi et al., 2007).

3.2 Analysis Method and Analysis Cases

For the 3D seismic response analysis, a dynamic elastic FEM is used as the numerical analysis method. This FEM enables a large-scale numerical computation with limited computing cost to be performed by combining structured grids and unstructured grids (Dobashi et al., 2007; Ichimura, Hori & Kuwamoto, 2007).

Meshes are generated so that numerical accuracy is assured up to the frequency of the primary mode of the ground. Ten elements per wavelength are used, and the resulting element size is shown in Table 2. An example of generated meshes is shown in Figure 5.

Figure 3 presents the four design earthquake ground motions. The wave at the bottom surface of the model is computed by using a draw-back method which uses the abovementioned one-dimensional equivalent linear analysis. Each input earthquake ground motion is inputted in the tunnel axial direction as well as in the direction perpendicular to the tunnel axis. The eight cases shown in Table 3(a) are analyzed. The duration of the analysis is 10.24 seconds, which includes the major motion of the strong ground motion, and the time increment is 0.01 second.

To clarify the 3D behavior of the tunnel system, a 2D model is made at each of the sections (a) to (c) of the 3D model shown in Figure 4. The plane strain state is assumed, but other conditions such as the model dimensions, boundary conditions and analysis constant are set identically to those in the 3D analysis. The parameters used in the 2D analysis are summarized in Table 3(b). Earthquake ground motion T1-B-2 is input in the direction perpendicular to the tunnel axis.

Table 2 Element Division of the Analytical Model

Input earthquake ground motion	Upper limit frequency of analytical accuracy assureance(Hz)	Element size		Number of nodes	Number of elements
		Unstructured grid (Tetrahedral element)	Structured grid (Cubic element)		
Level 1	4.0	7.0m (2nd order element)	3.5m (1st order element)	1,024,273	718,488
Level 2	3.0	1.75m (1st order element)	1.75m (1st order element)	1,474,016	4,182,054

Table 3 Analysis Cases

(a) 3D analysis cases

Input eqrthquake ground motion \ Input direction		X direction	Y direction
Level 1	L1-B-1	L1-B-1-X	L1-B-1-Y
	L1-B-2	L1-B-2-X	L1-B-2-Y
Level 2	T1-B-2	T1-B-2-X	T1-B-2-Y
	T2E-B-3	T2E-B-3-X	T2E-B-3-Y

(b) 2D analysis cases *1

Input earthquake ground motion		Input direction	Analytical cross section *2
Level 2	T1-B-2	Y direction	Section (a)
			Section (b)
			Section (c)

Notes:

*1: The reference case of 2D analysis is T1-B-2-Y in the 3D analysis.

*2: Refer to Figure 4 for the section location

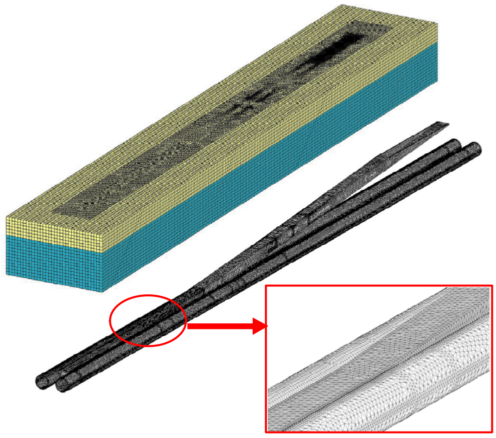

Figure 5 Example of FE Mesh for Analysis
(In Case of Level 1 Earthquake Ground Motion)

4. RESULTS OF ANALYSIS

4.1 3D Seismic Behavior of the Ramp Tunnel

Snapshots of the ramp tunnel deformation subjected to Level 1 and Level 2 earthquake ground motions are presented. The snapshots are taken at the time when the maximum relative displacement between the surface and the interface occurs. For example, the tunnel displacement distribution for L1-B-1 is shown in Figure 6(a) for input in the axial direction and Figures 6-(b) to (d) for input in the direction perpendicular to the axis. Similarly, the results for T1-B-2 are shown in Figures 7-(a) to (d). In all the cases, the response is small for the main tunnel and for the divergence/confluence part which is located in hard ground, while the response is large at the exit/entrance tunnel in the vicinity of the surface. As shown in Figures 6-(a) and 7-(a), when earthquake ground motion impinges in the axial direction of the tunnel (x direction), tensile and compressive strain occur at the exit/entrance tunnel in the direction of earthquake ground motion input. On the other hand, as shown in Figures 6-(b) to (d) and 7-(b) to (d), when seismic force acts in the direction perpendicular to the tunnel axis (y direction), the axial displacement component (x displacement) and the perpendicular displacement component (z displacement) increase, in addition to the displacement component in the direction of the input earthquake ground motion (y displacement). This is due to the occurrence of bending and torsion that are caused by the rotation in the longitudinal direction at the exit/entrance tunnel.

A comparison of Figure 6 with Figure 7 clearly shows that the 3D response increases remarkably when Level 2 earthquake ground motion is input instead of Level 1 motion. The distribution of response displacement differs significantly for these two earthquakes. For instance, Figures 6-(c) and 7-(c) reveal that the axial displacement component smoothly changes when Level 1 earthquake ground motion is input, while in the case of Level 2 motion, the response is concentrated at the exit/entrance tunnel, slightly up at the interface of the two layers.

To compare the ramp tunnel responses subjected to different earthquake ground motions, the distribution of response displacement in the direction of earthquake ground motion, at the instant when the relative displacement between the surface and the interface becomes the maximum, is shown in Figure 8 for all eight cases. Out of the four earthquake ground motions, the response caused by T1-B-2 shows a different trend compared with the other cases. This implies that the seismic response of the ramp tunnel changes depending on the input earthquake ground motion. For example, in the case of input in the direction perpendicular to the tunnel axis, Y-direction response displacement becomes the maximum in the vicinity of X = 550 m, which is the location at the exit/entrance tunnel where the depth of overburden is approximately 3 m in the first layer. On the other hand, the closer to the surface, the larger the response at the exit/entrance tunnel becomes compared with other earthquake ground motions.

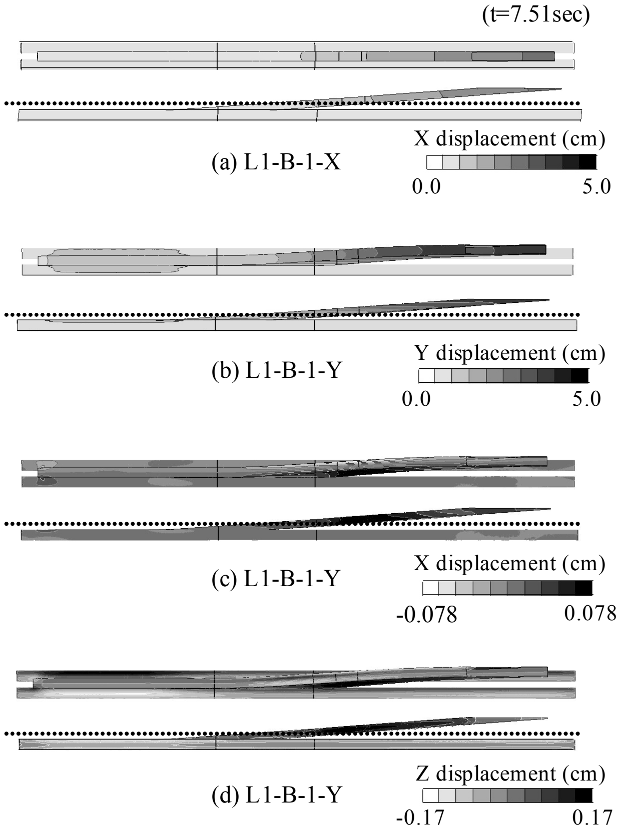

Figure 6 Distribution of Response Displacement for the Tunnel (L1-B-1)
(Upper figure: plane view; lower figure: side view)

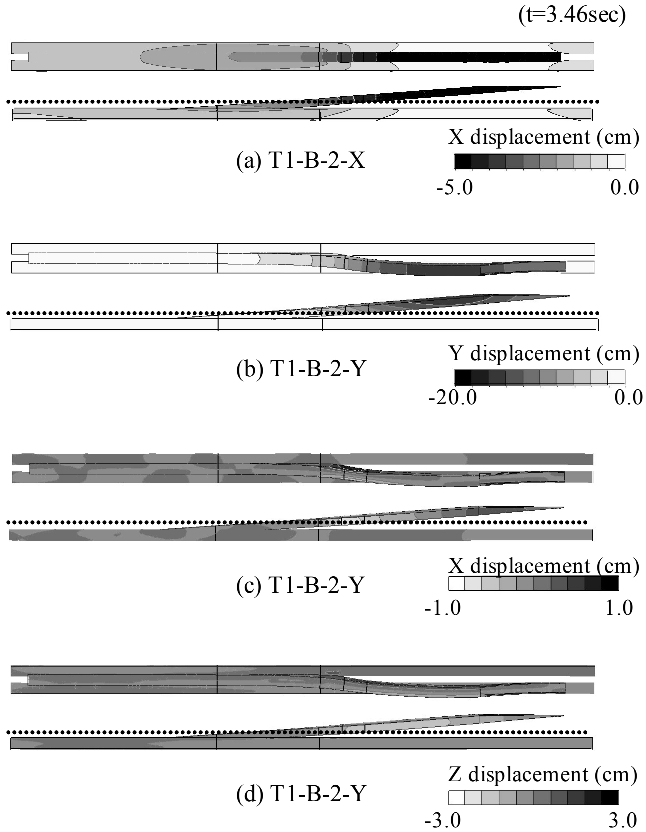

Figure 7 Distribution of Response Displacement for the Tunnel (T1-B-2)
(Upper figure: plane view; lower figure: side view)

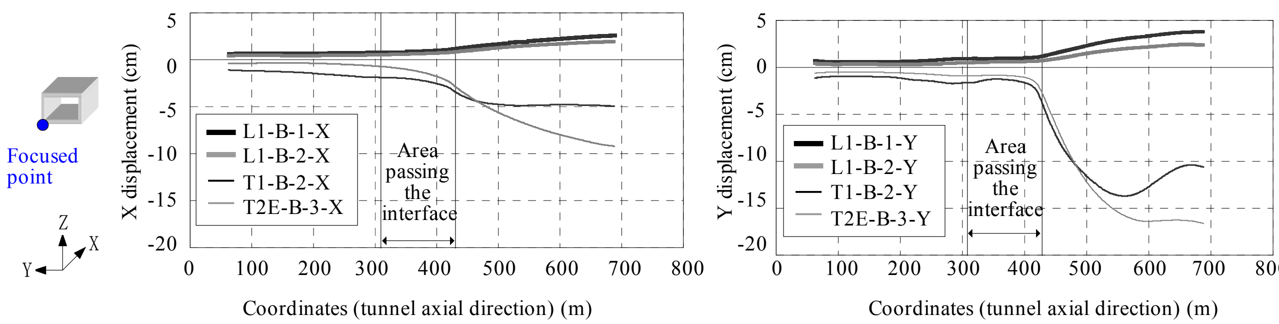

(a) Input in the tunnel axial direction

(b) Input in the direction perpendicular to tunnel axis

Figure 8 Distribution of Response Displacement for the Ramp Tunnel by Input Direction of Earthquake Ground Motion

4.2 Effects of 3D Analysis of Seismic Behavior

Focusing on the response displacement at the corners of the ramp tunnel structure, Figure 9 compares the results of the 3D analysis with those of the 2D analysis for T1-B-2 in the direction perpendicular to the tunnel axis. Note that the response displacement at the corners obtained by the 3D and 2D analyses agree well with each other for Section (a) which is located in the second layer or hard ground, while the response displacement does not agree for Sections (b) and (c) where the tunnel is located in the soft first layer.

As for the maximum displacement of Section (c), 20.4 cm is obtained by the 3D analysis while 15.3 cm by the 2D analysis: the 2D analysis underestimates the displacement by approximately 25 % compared with the 3D analysis. Similarly, for Section (b), the overestimate of the maximum displacement is approximately 11 %. On the other hand, regarding the minimum displacement of Section (c), –16.3 cm and –18.6 cm are obtained by the 3D and 2D analyses, resulting in an overestimate of approximately 14 % by the 2D analysis. The minimum displacement at Section (b) is underestimated by approximately 5 %. This leads to another inconsistency in values between the two analyses. Also, the maximum response displacement occurs at different time steps between the two analyses.

Figure 10 illustrates the deformation of Section (b) obtained by the 3D analysis and the 2D analysis, at the time of 3.46 seconds, which is when the ground response of the free field reaches the maximum. Judging from the time history, the response displacement of the ramp tunnel differs between the 2D analysis and the 3D analysis, although the deformation modes at the section are similar to each other. Figure 11 compares the relative displacement between the upper and bottom slabs of the ramp tunnel at the same section. Similar to the tendency of the response displacement, both the peak value and time of occurrence of relative displacement differ between the 3D analysis and the 2D analysis.

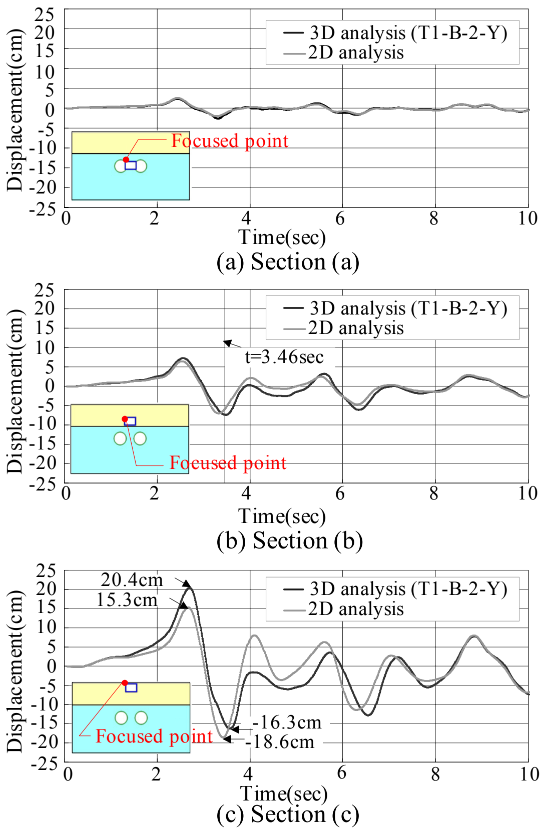

(a) Section (a)
(b) Section (b)
(c) Section (c)

Figure 9 Comparison of 3D Analysis and 2D -Analysis Time Series of Response Displacements-

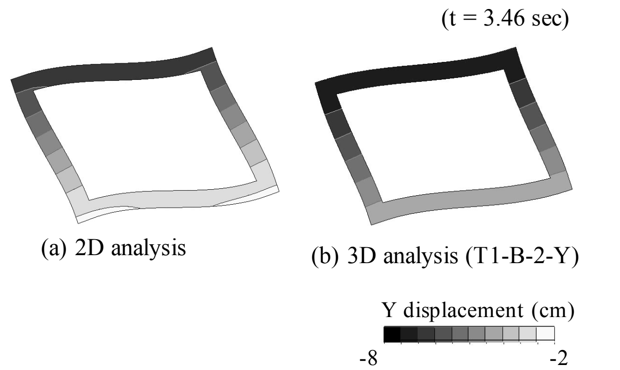

(a) 2D analysis
(b) 3D analysis (T1-B-2-Y)

Figure 10 Comparison of 3D Analysis and 2D Analysis -Deformation of Section (b)-

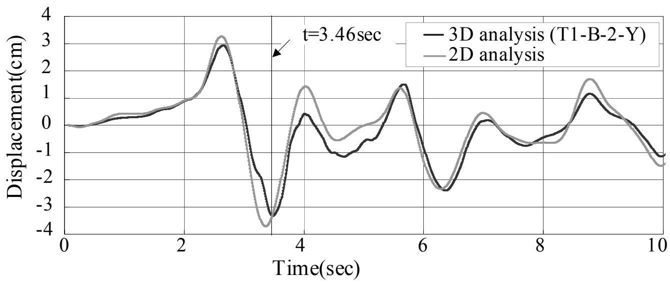

Figure 11 Comparison of 3D Analysis and 2D Analysis -Relative Displacement of Upper and Bottom Slabs of the Ramp Tunnel-

5. RESULTS

The results of the present study can be summarized as follows.

3D seismic behavior of the ramp tunnel:
The seismic behavior of the ramp tunnel has the following characteristics.

i) Tunnel seismic response is small for the main tunnel and the divergence/confluence part which is located in hard ground.
ii) Upon receiving seismic force in the tunnel axial direction, compression or tension occurs in the exit/entrance tunnel, while upon receiving seismic force in the direction perpendicular to the tunnel axis, the ramp tunnel is shaken horizontally, and bending and rotation-associated torsion occur in the longitudinal direction.
iii) For the ramp tunnel which has a large structure and is located at increasing depth, the seismic response has large variations depending on the characteristics of the input earthquake ground motion such as acceleration and frequency.

3D nature of seismic behavior:
The 3D nature of the seismic response which cannot be computed by a 2D analysis was quantitatively evaluated by a 3D analysis. The results of the 3D analysis and the 2D analysis were compared for the case when the earthquake ground motion is perpendicular to the tunnel axis, and the following findings were obtained:

i) The 2D analysis and 3D analysis obtain different responses for the ramp tunnel which is located in soft ground, and the difference in response varies depending on the location.
ii) The results of the 2D analysis and 3D analysis generally agree with each other for the divergence/ confluence part which is located in hard ground.

6. CONCLUSION

This study confirmed the complexity of the seismic behavior of the ramp tunnel by using large-scale numerical computation of the actual tunnel. The 3D behavior of the tunnel was clarified by comparing the 2D and 3D analyses. This comparison also revealed the 3D nature of the seismic response of the structure, which cannot be evaluated by current design methods based on 2D analyses. In the future, it is desirable to examine such 3D responses and to carry out an extensive comparative study between the results of the current design methods and the results of a 3D analysis.

REFERENCES

The Act on Temporary Measures concerning Public Use of the Deep Underground. Law No. 87, enacted on May 26, 2000 and revised on July 24, 2003 as Law No. 125.

Ohbo, N., Horikoshi, K., Yamada, T., Tachibana, K. and Akiba, H. (2004). Dynamic Behavior of an Underground Motorway Junction due to Large Earthquake, 13th World Conference on Earthquake Engineering, paper No. 1215.

Dobashi, H., Ochiai, E., Ichimura, T., Yamada, T., Yamaki, Y., Ohbo, N., Moriguchi, M., Itami, H. and Hori, M. (2007). 3D FE Analysis of Seismic Response of Complicated Large-Scale Ramp Tunnel Structure. ECCOMAS Thematic Conference on Computational Methods in Structural Dynamics and Earthquake Engineering, Rethymno, Crete, Greece, 13–16 June 2007.

Ichimura, T., Hori, M. and Kuwamoto, H. (2007). Earthquake Motion Simulation with Multi-Scale Finite Element Analysis on Hybrid Grid. Bulletin of the Seismological Society of America 97:4, 1133–1143, DOI: 10.1785/0120060175.